

VARIABLE GAMMA-RAY SKY AT 1 GeV

M. S. Pshirkov^{a,b,c*}, G. I. Rubtsov^{b,d}

^a Sternberg Astronomical Institute, Lomonosov Moscow State University
119991, Moscow, Russia

^b Institute for Nuclear Research, Russian Academy of Sciences
117312, Moscow, Russia

^c Pushchino Radio Astronomy Observatory of Lebedev Physical Institute, Russian Academy of Sciences
142290, Pushchino, Moscow Region, Russia

^d Novosibirsk State University
630090, Novosibirsk, Russia

Received July 5, 2012

We search for the long-term variability of the gamma-ray sky in the energy range $E > 1$ GeV with 168 weeks of the gamma-ray telescope Fermi-LAT data. We perform a full sky blind search for regions with variable flux looking for deviations from uniformity. We bin the sky into 12288 pixels using the HEALPIX package and use the Kolmogorov-Smirnov test to compare weekly photon counts in each pixel with the constant flux hypothesis. The weekly exposure of Fermi-LAT for each pixel is calculated with the Fermi-LAT tools. We consider flux variations in a pixel significant if the statistical probability of uniformity is less than $4 \cdot 10^{-6}$, which corresponds to 0.05 false detections in the whole set. We identified 117 variable sources, 27 of which have not been reported variable before. The sources with previously unidentified variability contain 25 active galactic nuclei (AGN) belonging to the blazar class (11 BL Lacs and 14 FSRQs), one AGN of an uncertain type, and one pulsar PSR J0633+1746 (Geminga).

DOI: 10.7868/S0044451013010070

1. INTRODUCTION

Time domain astronomy at different wavelengths, from radio to very high-energy gamma rays, is currently developing very rapidly. In the high-energy (HE) range (≥ 100 MeV), great progress was achieved with the advent of the gamma-ray telescope Fermi-LAT [1]. Its high sensitivity and almost uniform sky coverage allow studying the variability of a large number of sources at these energies on time scales from seconds to years. Sources that demonstrate the most variable behavior are active galactic nuclei (AGN), primarily of the blazar type [2]. It is well known that these sources exhibit variability on different time scales and at different wavelengths [3–12]. Studies of the time variability of these sources are very important for better understanding the AGN engines; they are also essential for assessing the quality of spectral energy distributions

obtained from multiwavelength observations made at different epochs.

In this paper, we perform a full sky blind search for variable sources. We bin the sky into equal-area pixels and search for deviations of photon number counts from the uniformity in time.

2. DATA AND METHOD

The LAT Pass 7 weekly all-sky data publicly available at the Fermi mission website¹⁾ were used in this work. The analysis covers the time period of 168 weeks from August 04, 2008 to October 18, 2011, corresponding to the mission elapsed time (MET) from 239557417 s to 340622181 s. We use the “Pass 7 Source” event class photons with $E > 1$ GeV and impose an Earth relative zenith angle cut of 100° and rocking angle cut of 52° .

We bin the data week by week using the HEALPIX package [13] into a map of resolution $N_{side} = 32$ in galactic coordinates with the “RING” pixel ordering.

*E-mail: pshirkov@gmail.com

¹⁾ <http://fermi.gsfc.nasa.gov/ssc/data/access/>

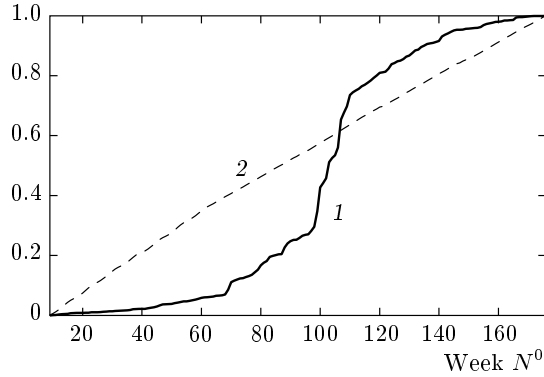


Fig. 1. Plot of the cumulative functions $\mathcal{P}(t)$ (1) and $\mathcal{E}(t)$ (2) for pixel № 54 ($l = 261^\circ$, $b = 82.^\circ69$). The difference can be easily seen, and the probability that the photon rate is constant is only $P = 4 \cdot 10^{-80}$

The total number of pixels is equal to 12288 and the area of each pixel is 3.6 sq.deg, chosen according to the size of the Fermi-LAT point-spread function (PSF) above 1 GeV, which is approximately 1° . We estimate the integral weekly exposure for each pixel using the standard Fermi-LAT tools “gtlcube” and “gtexpcube” (ScienceTools-v9r23p1-fssc-20110726).

For each pixel, we count the number of photons in each of the 168 weeks and consider the corresponding values of weekly exposure. Typically, there are 2–10 photons in a pixel per week except pixels with the brightest sources. Cumulative distribution functions (CDFs) $\mathcal{P}(t)$ and $\mathcal{E}(t)$ for both photon counts and exposure are constructed. In the absence of variability, the photon counts would represent a random process with the CDF proportional to $\mathcal{E}(t)$, and therefore $\mathcal{P}(t)$ would follow $\mathcal{E}(t)$ with deviations caused by a finite number of observed photons. Otherwise, $\mathcal{P}(t)$ would not be statistically compatible with $\mathcal{E}(t)$. The Kolmogorov-Smirnov (KS) test is a natural and straightforward way to examine statistical compatibility of the observed photon counts with the distribution given by the CDF $\mathcal{E}(t)$. The probability that both sets represent the same distribution can be estimated from the maximal value of the distance between the functions $\mathcal{P}(t)$ and $\mathcal{E}(t)$. An example CDFs for one of the pixels is shown in Fig. 1 and the corresponding flux is shown in Fig. 2.

The implemented KS test is most sensitive to the variability at long scales (longer than a week), while transient bursts and flares at shorter time scales may be missed if they are not overwhelmingly strong. On the other hand, our method is sensitive to gradual moderate changes in photon fluxes without any prominent bursts, which could be missed by burst searching techniques.

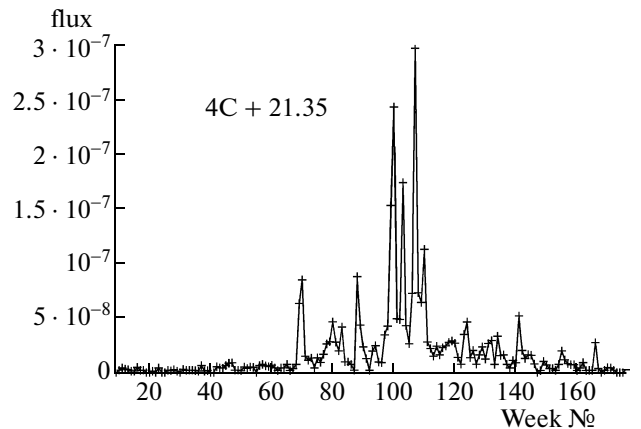


Fig. 2. The flux of photons with energies larger than 1 GeV for pixel № 54 (4C+21.35, see Fig. 1). The flux is in $\text{photons} \cdot \text{cm}^{-2} \cdot \text{s}^{-1}$ units

The KS probability is calculated for each pixel, we are interested in pixels with probabilities smaller than the threshold value $P_0 = 4 \cdot 10^{-6}$. This threshold value is set to allow for penalty coming from the large number ($N_{pix} = 12288$) of trials: the detection criterion is chosen in such a way that the entire search would give a single false detection with the probability

$$P_0 N_{pix} \approx 0.05.$$

A map of the probabilities is presented in Fig. 3.

3. RESULTS

The total number of pixels with probabilities smaller than the threshold value P_0 is 151. The source identification for each of these pixels is performed as follows. We consider the photons that arrived during several weeks at the epoch of the maximal flux. The center of mass of the spatial distribution of these photons is used as an initial estimate of the source location. We search for sources from the 2FGL [14] catalog in the circle with a radius equal to the error of the center-of-mass estimation, which is usually about $10'-15'$ for approximately 20 photons). For 34 pixels, no source is found with the initial estimate: in 31 of them, the variability time pattern and photon spatial distribution lead us to the identification of the source located in the neighbouring pixel and already identified there. In three cases (pixels 2877 and 2749, PMN J1532-1315, and pixel 2299, SBS 0846+513), we have found no counterpart in the 2FGL catalog and used the Simbad astronomical database. Gamma-ray

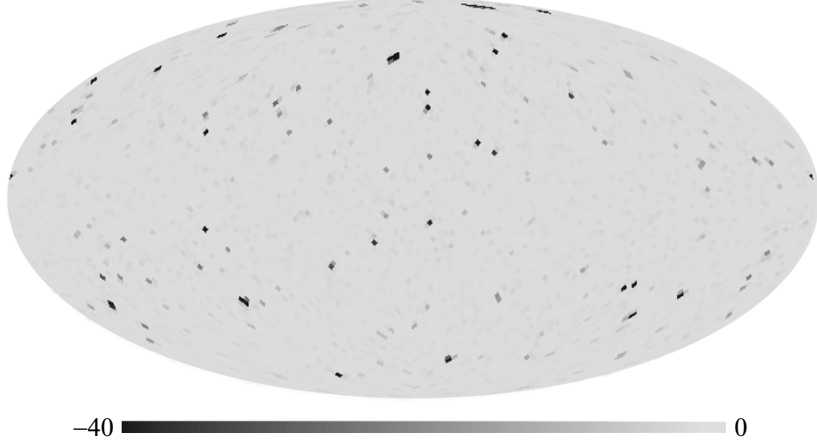


Fig. 3. Map of the Fermi-LAT variability at 1 GeV in galactic coordinates. Pixel color represents base-10 logarithm of the Kolmogorov–Smirnov probability of the uniformity of the observed flux. The galactic center is at the center of the figure, $l = 180^\circ$ is on the left

flares from the latter two sources (PMN J1532-1315 and SBS 0846+513) have been recently reported by Fermi-LAT [15, 16], but the activity period is outside the time region of the 2FGL catalog. To avoid false identifications, we performed an additional check in four cases where two different sources were residing in adjacent pixels: a significant difference in the observed luminosity curves confirms that these detections are real. The results are presented in Table 1. The table columns l, b are the galactic coordinates of the center of the pixel, N_{phot} is the total number of photons observed in the pixel, Φ_{-8} is the average flux from the pixel in units of 10^{-8} photons·cm $^{-2} \cdot$ s $^{-1}$, and P is the KS probability. The notations for the identified source in the literature and in the 2FGL catalog are in the 8th and 9th columns. Previous references to the variability of the source are presented in the last column: P stands for paper [2], P2 for [17], P3 for [18], ATNNNN for ATel #NNNN, and BNnn indicates that the outburst from the source was mentioned on the Fermi blog in the NNNth weekly report. ATNNNN with a prefix VHE or IR indicates that a flare was observed (and reported in the corresponding ATel) in some other energy range: at a very high energy (larger than 100 GeV) or in the infrared. All the references for the ATels are listed in the Appendix.

The total number of identified sources is 117; variability of 55 of them was reported in [2, 17, 18], 35 additional detections were made in numerous Astronomers's telegrams (ATels; see the Appendix) and on the Fermi-

LAT blog²⁾. That leaves us with 27 sources for which the variability has not been previously detected (see Table 2). We have explicitly checked that the flux from these sources is not contaminated with the contribution from the Sun.

For convenience, we assign a variability type to the source: a gradual change in the photon flux is referred to as “rate”, if the whole variability is dominated by one or several flares, we call it a “flare”, and if these flares are observed over a more or less prolonged time span (typically, more than 20 weeks), we designate it as “activity”. This morphological distinction is not totally unambiguous: several bright consequent flares could be defined as “activity”. On the other hand, gradual changes could occur on time scales of several dozens of weeks, thus fitting the “activity” type as well.

The BL Lacs and the flat-spectrum radio quasars (FSRQs) are represented almost equally in the set of previously unidentified sources: there are 11 BL Lacs, 14 FSRQs, and one AGN of uncertain type (PKS 0644-671). Also, there is one pulsar (Geminga) in the list (see Table 2 and Fig. 4). Both BL Lacs and FSRQs demonstrate two types of variability: gradual change of the photon flux (10 out of 25) and flares or increased activity (15 out of 25). The variability of several sources was observed before in other energy ranges: a flare in the near-infrared region was observed for B2 1732+38A (ATel #3504 [19], 1 July 2011), VHE flares of 1ES0806+524 were observed by MAGIC (ATel #3192 [20], 24 February 2011), and EGRET observed

²⁾ <http://fermisky.blogspot.com/>

Table 1. List of pixels demonstrating variability exceeding the threshold value. See text for description

Nº	Pixel Nº	l°	b°	N_{phot}	Φ_{-8}	P	Source	2FGL	Ref.
1	23	345.0	85.6	264	0.29	$2.8 \cdot 10^{-13}$	MG2 J130304+2434	J1303.1+2435	AT2110
2	44	81.0	82.7	454	0.48	$6.5 \cdot 10^{-14}$	OP 313	J1310.6+3222	P
3	51	207.0	82.7	467	0.50	$1.4 \cdot 10^{-6}$	W Comae	J1221.4+2814	P
4	54	261.0	82.7	1700	1.86	$4.3 \cdot 10^{-80}$	4C+21.35	J1224.9+2122	P2
5	66	97.5	81.2	194	0.20	$3.9 \cdot 10^{-6}$	5C 12.291	J1308.5+3547	
6	76	247.5	81.2	935	1.02	$2.4 \cdot 10^{-159}$	4C+21.35	J1224.9+2122	P2
7	77	262.5	81.2	475	0.52	$1.3 \cdot 10^{-27}$	4C+21.35	J1224.9+2122	P2
8	103	250.7	79.7	216	0.23	$1.4 \cdot 10^{-6}$	4C +21.35	J1224.9+2122	P2
9	129	196.9	78.3	783	0.84	$7.7 \cdot 10^{-40}$	Ton 599	J1159.5+2914	P
10	335	162.7	70.9	468	0.48	$1.9 \cdot 10^{-16}$	S4 1144+40	J1146.9+4000	B165
11	373	61.1	69.4	188	0.20	$1.8 \cdot 10^{-9}$	J1424+3615	J1424+3615	
12	378	93.2	69.4	332	0.33	$4.2 \cdot 10^{-10}$	B3 1343+451	J1345.4+4453	AT3793
13	381	112.5	69.4	433	0.43	$1.9 \cdot 10^{-11}$	GB 1310+487	J1312.8+4828	AT2316
14	438	111.0	67.9	343	0.33	$2.1 \cdot 10^{-22}$	GB 1310+487	J1312.8+4828	AT2316
15	532	295.3	66.4	461	0.54	$7.3 \cdot 10^{-9}$	MG1 J123931+0443	J1239.5+0443	AT3445
16	564	108.5	64.9	201	0.19	$1.4 \cdot 10^{-7}$	CLASS J1333+5057	J1333.5+5058	
17	571	145.6	64.9	370	0.36	$7.5 \cdot 10^{-61}$	OM 484	J1153.2+4935	B153
18	598	288.5	64.9	855	1.00	$3.3 \cdot 10^{-56}$	3C 273	J1229.1+0202	P
19	670	292.5	63.4	301	0.35	$2.1 \cdot 10^{-6}$	3C 273	J1229.1+0202	P
20	998	304.8	57.4	1925	2.26	$5.1 \cdot 10^{-57}$	3C 279	J1256.1-0547	P
21	1014	9.8	55.9	967	1.10	$6.3 \cdot 10^{-123}$	PKS 1502+106	J1504.3+1029	P
22	1106	9.4	54.3	598	0.68	$2.0 \cdot 10^{-62}$	PKS 1502+106	J1504.3+1029	P
23	1107	13.1	54.3	1414	1.60	$4.1 \cdot 10^{-212}$	PKS 1502+106	J1504.3+1029	P
24	1159	208.1	54.3	443	0.48	$3.4 \cdot 10^{-11}$	MG2 J101241+2439	J1012.6+2440	P
25	1203	12.6	52.8	358	0.41	$4.1 \cdot 10^{-24}$	PKS 1502+106	J1504.3+1029	P
26	1448	148.3	49.7	744	0.64	$3.5 \cdot 10^{-60}$	S4 1030+61	J1033.9+6050	P
27	1483	265.0	49.7	321	0.38	$2.0 \cdot 10^{-10}$	PKS 1118-05	J1121.5-0554	B71
28	1499	318.3	49.7	310	0.36	$8.1 \cdot 10^{-7}$	PMN J1332-1256	J1332.5-1255	
29	1585	236.2	48.1	267	0.31	$3.0 \cdot 10^{-12}$	PMN J1016+0512	J1016.0+0513	P
30	1631	23.3	46.6	374	0.42	$7.6 \cdot 10^{-10}$	PKS 1551+130	J1553.5+1255	P
31	1654	94.7	46.6	465	0.40	$1.4 \cdot 10^{-9}$	GB6 J1542+6129	J1542.9+6129	P
32	1700	237.4	46.6	283	0.33	$3.3 \cdot 10^{-12}$	PMN J1016+0512	J1016.0+0513	P
33	1798	175.5	45.0	729	0.73	$1.2 \cdot 10^{-44}$	S4 0917+44	J0920.9+4441	P
34	1970	320.8	43.4	538	0.62	$8.3 \cdot 10^{-15}$	PMN J1344-1723	J1344.2-1723	
35	2005	60.5	41.8	1193	1.23	$2.7 \cdot 10^{-22}$	4C+38.41	J1635.2+3810	P
36	2006	63.3	41.8	808	0.82	$1.7 \cdot 10^{-6}$	NRAO 512	J1640.7+3945	P3
37	2237	351.6	40.2	2977	3.47	$1.5 \cdot 10^{-61}$	PKS 1510-08	J1512.8-0906	P
38	2299	167.3	38.7	276	0.26	$8.1 \cdot 10^{-13}$	SBS 0846+513		AT3452

Nº	Pixel №	l°	b°	N_{phot}	Φ_{-8}	P	Source	2FGL	Ref.
39	2338	277.0	38.7	527	0.60	$2.4 \cdot 10^{-33}$	PKS 1124-186	J1126.6-1856	AT3207
40	2392	67.5	37.2	254	0.25	$1.1 \cdot 10^{-7}$	B3 1708+433	J1709.7+4319	AT3026
41	2475	300.9	37.2	940	1.06	$1.4 \cdot 10^{-11}$	PKS 1244-255	J1246.7-2546	P
42	2520	68.9	35.7	498	0.50	$1.9 \cdot 10^{-26}$	B3 1708+433	J1709.7+4319	AT3026
43	2569	206.7	35.7	551	0.60	$8.9 \cdot 10^{-12}$	OJ 287	J0854.8+2005	P
44	2683	165.9	34.2	258	0.24	$4.7 \cdot 10^{-7}$	1ES 0806+524	J0809.8+5218	VHE AT3192
45	2749	351.6	34.2	628	0.73	$1.4 \cdot 10^{-77}$	PMN J1532-1319		AT3579
46	2810	164.5	32.8	254	0.24	$1.9 \cdot 10^{-7}$	1ES 0806+524	J0809.8+5218	VHE AT3192
47	2811	167.3	32.8	537	0.51	$9.6 \cdot 10^{-16}$	1ES 0806+524	J0809.8+5218	VHE AT3192
48	2815	178.6	32.8	735	0.74	$1.2 \cdot 10^{-6}$	S4 0814+42	J0818.2+4223	P
49	2844	260.2	32.8	290	0.33	$1.3 \cdot 10^{-7}$	1RXS J102658.5-174905	J1026.7-1749	
50	2877	353.0	32.8	431	0.50	$3.9 \cdot 10^{-15}$	PMN J1532-1319		AT3579
51	2903	64.7	31.4	404	0.41	$2.1 \cdot 10^{-16}$	B2 1732+38A	J1734.3+3858	IR AT3504
52	2916	101.2	31.4	466	0.38	$9.2 \cdot 10^{-21}$	S4 1749+70	J1748.8+7006	AT3171
53	3043	99.8	30.0	830	0.67	$4.0 \cdot 10^{-8}$	S4 1749+70	J1748.8+7006	AT3171
54	3150	39.4	28.6	371	0.40	$1.9 \cdot 10^{-21}$	PKS 1717+177	J1719.3+1744	P
55	3187	143.4	28.6	1845	1.49	$4.0 \cdot 10^{-10}$	S5 0716+71	J0721.9+7120	P
56	3194	163.1	28.6	756	0.69	$1.7 \cdot 10^{-50}$	GB6 J0742+5444	J0742.6+5442	AT3445
57	3246	309.4	28.6	451	0.50	$2.7 \cdot 10^{-10}$	PKS 1313-333	J1315.9-3339	B122
58	3489	272.8	25.9	247	0.28	$1.3 \cdot 10^{-7}$	PKS B1043-291	J1045.5-2931	
59	3540	57.7	24.6	557	0.58	$1.1 \cdot 10^{-16}$	RX J1754.1+3212	J1754.3+3212	
60	3554	97.0	24.6	896	0.73	$1.1 \cdot 10^{-50}$	S4 1849+67	J1849.4+6706	P
61	3598	220.8	24.6	439	0.50	$1.4 \cdot 10^{-7}$	PKS 0829+046	J0831.9+0429	
62	3963	165.9	20.7	462	0.44	$5.9 \cdot 10^{-9}$	GB6 J0654+5042	J0654.5+5043	P
63	4000	270.0	20.7	325	0.36	$1.7 \cdot 10^{-15}$	PKS 1021-323	J1023.8-3248	
64	4021	321.1	20.7	813	0.90	$1.8 \cdot 10^{-44}$	PKS 1454-354	J1457.4-3540	P
65	4092	170.2	19.5	457	0.45	$5.9 \cdot 10^{-10}$	B3 0650+453	J0654.2+4514	P
66	4097	184.2	19.5	613	0.64	$9.7 \cdot 10^{-8}$	B2 0716+33	J0719.3+3306	P
67	4110	220.8	19.5	324	0.37	$2.0 \cdot 10^{-8}$	OJ 014	J0811.4+0149	
68	4116	237.7	19.5	412	0.48	$5.7 \cdot 10^{-8}$	BZQ J0850-1213	J0850.2-1212	B102,114
69	4149	330.5	19.5	463	0.51	$2.6 \cdot 10^{-7}$	PKS 1454-354	J1457.4-3540	P
70	4402	322.0	17.0	1495	1.63	$7.8 \cdot 10^{-36}$	PKS B1424-418	J1428.0-4206	AT2104,2583
71	4541	351.6	15.7	1505	1.69	$1.5 \cdot 10^{-19}$	PKS 1622-253	J1625.7-2526	P
72	4614	198.3	14.5	338	0.37	$1.2 \cdot 10^{-6}$	MG2 J071354+1934	J0714.0+1933	P
73	4616	203.9	14.5	799	0.88	$4.0 \cdot 10^{-19}$	4C+14.23	J0725.3+1426	AT2243
74	4625	229.2	14.5	402	0.46	$1.1 \cdot 10^{-6}$	PKS 0805-07	J0808.2-0750	AT2048,2136
75	4742	196.9	13.2	413	0.44	$5.7 \cdot 10^{-17}$	MG2 J071354+1934	J0714.0+1933	P
76	4744	202.5	13.2	353	0.38	$1.9 \cdot 10^{-6}$	4C+14.23	J0725.3+1426	AT2243

Nº	Pixel №	l°	b°	N_{phot}	Φ_{-8}	P	Source	2FGL	Ref.
77	4753	227.8	13.2	707	0.82	$5.5 \cdot 10^{-16}$	PKS 0805-07	J0808.2-0750	AT2048,2136
78	4881	229.2	12.0	556	0.64	$3.4 \cdot 10^{-14}$	PKS 0805-07	J0808.2-0750	AT2048,2136
79	4932	11.2	10.8	1337	1.54	$2.7 \cdot 10^{-16}$	PKS 1730-13	J1733.1-1307	AT3002
80	5119	178.6	9.6	619	0.64	$9.9 \cdot 10^{-8}$	B2 0619+33	J0622.9+3326	AT2829
81	5165	308.0	9.6	1011	1.06	$2.6 \cdot 10^{-7}$	PMN J1326-5256	J1326.7-5254	
82	5637	195.5	4.8	52455	56.6	$2.3 \cdot 10^{-7}$	PSR J0633+1746	J0633.9+1746	
83	5248	180.0	8.4	1212	1.26	$1.1 \cdot 10^{-46}$	B2 0619+33	J0622.9+3326	AT2829
84	5777	227.8	3.6	2002	2.3	$3.2 \cdot 10^{-12}$	PKS 0727-11	J0730.2-1141	AT2860
85	6596	12.7	-4.8	1854	2.1	$4.6 \cdot 10^{-7}$	PKS 1830-211	J1833.6-2104	AT2943
86	6608	46.4	-4.8	1198	1.3	$3.6 \cdot 10^{-7}$	RX J1931.1+0937	J1931.1+0938	
87	6711	336.1	-4.8	1717	1.8	$2.6 \cdot 10^{-9}$	PMN J1650-5044	J1650.1-5044	
88	6724	11.2	-6.0	1945	2.2	$2.9 \cdot 10^{-15}$	PKS 1830-211	J1833.6-2104	AT2943
89	7101	351.6	-8.4	1553	1.71	$5.4 \cdot 10^{-38}$	PMN J1802-3940	J1802.6-3940	
90	7155	144.8	-9.6	696	0.67	$3.4 \cdot 10^{-7}$	4C+47.08	J0303.5+4713	
91	7265	92.8	-10.8	1664	1.65	$1.9 \cdot 10^{-46}$	BL Lac	J2202.8+4216	P
92	7413	150.5	-12.0	931	0.93	$1.2 \cdot 10^{-8}$	NGC 1275	J0319.8+4130	P
93	7494	16.9	-13.2	868	0.98	$1.2 \cdot 10^{-7}$	PKS B1908-201	J1911.1-2005	P
94	7542	151.9	-13.2	1202	1.21	$6.7 \cdot 10^{-9}$	NGC 1275	J0319.8+4130	P
95	7569	227.8	-13.2	539	0.61	$2.3 \cdot 10^{-8}$	PKS 0627-199	J0629.3-2001	B174
96	7662	130.8	-14.5	868	0.84	$9.1 \cdot 10^{-23}$	OC 457	J0136.9+4751	P
97	7750	16.9	-15.7	801	0.91	$7.5 \cdot 10^{-36}$	TXS 1920-211	J1923.5-2105	P
98	7921	139.2	-17.0	2228	2.2	$3.6 \cdot 10^{-10}$	3C 66A	J0222.6+4302	P
99	7993	341.7	-17.0	512	0.54	$3.5 \cdot 10^{-6}$	PKS 1821-525	J1825.1-5231	
100	8030	84.4	-18.2	677	0.70	$5.8 \cdot 10^{-17}$	B2 2155+31	J2157.4+3129	P
101	8197	195.5	-19.5	896	1.01	$4.9 \cdot 10^{-20}$	TXS 0506+056	J0509.4+0542	
102	8525	36.6	-23.3	431	0.50	$8.0 \cdot 10^{-16}$	PKS 2023-07	J2025.6-0736	P
103	8653	38.0	-24.6	563	0.65	$1.3 \cdot 10^{-31}$	PKS 2023-07	J2025.6-0736	P
104	8675	99.8	-24.6	658	0.68	$4.8 \cdot 10^{-23}$	B2 2308+34	J2311.0+3425	AT2783
105	8867	278.4	-25.9	508	0.50	$1.1 \cdot 10^{-13}$	PKS 0644-671	J0644.2-6713	
106	9074	140.6	-28.6	428	0.44	$1.4 \cdot 10^{-17}$	B2 0200+30	J0204.0+3045	B134
107	9077	149.1	-28.6	821	0.86	$1.2 \cdot 10^{-31}$	4C+28.07	J0237.8+2846	AT3670
108	9094	196.9	-28.6	466	0.53	$1.6 \cdot 10^{-22}$	PKS 0440-00	J0442.7-0017	AT2049
109	9197	128.0	-30.0	512	0.53	$1.1 \cdot 10^{-17}$	4C 31.03	J0112.8+3208	
110	9369	250.3	-31.4	3416	3.67	$1.6 \cdot 10^{-90}$	PKS 0537-441	J0538.8-4405	P
111	9431	66.1	-32.8	395	0.44	$1.1 \cdot 10^{-8}$	PKS 2144+092	J2147.3+093	P
112	9477	195.5	-32.8	588	0.67	$1.9 \cdot 10^{-15}$	PKS 0420-01	J0423.2-0120	AT2402
113	9498	254.5	-32.8	946	1.01	$7.7 \cdot 10^{-101}$	PMN J0531-4827	J0532.0-4826	AT2907
114	9615	222.2	-34.2	259	0.30	$3.6 \cdot 10^{-8}$	PKS 0454-234	J0457.0-2325	P

Nº	Pixel №	l°	b°	N_{phot}	Φ_{-8}	P	Source	2FGL	Ref.
115	9616	225.0	-34.2	341	0.38	$7.5 \cdot 10^{-14}$	PKS 0454-234	J0457.0-2325	P
116	9743	223.6	-35.7	1282	1.43	$5.8 \cdot 10^{-18}$	PKS 0454-234	J0457.0-2325	P
117	9776	316.4	-35.7	483	0.50	$2.4 \cdot 10^{-17}$	PKS 2142-75	J2147.4-7534	AT2539
118	9822	84.4	-37.2	782	0.85	$5.2 \cdot 10^{-23}$	3C 454.3	J2253.9+1609	P
119	9823	87.2	-37.2	1832	1.98	$1.5 \cdot 10^{-72}$	3C 454.3	J2253.9+1609	P
120	9904	315.0	-37.2	530	0.55	$1.8 \cdot 10^{-15}$	PKS 2142-75	J2147.4-7534	AT2539
121	9947	77.3	-38.7	500	0.55	$4.2 \cdot 10^{-13}$	CTA 102	J2232.4+1143	P
122	9951	88.6	-38.7	417	0.45	$1.8 \cdot 10^{-6}$	3C 454.3	J2253.9+1609	P
123	9950	85.8	-38.7	10048	11.0	$7.4 \cdot 10^{-539}$	3C 454.3	J2253.9+1609	P
124	9975	156.1	-38.7	1097	1.19	$7.5 \cdot 10^{-247}$	AO 0235+164	J0238.7+1637	P
125	10094	129.4	-40.2	838	0.89	$4.4 \cdot 10^{-8}$	S2 0109+22	J0112.1+2245	P
126	10104	157.5	-40.2	522	0.57	$4.0 \cdot 10^{-37}$	AO 0235+164	J0238.7+1637	P
127	10108	168.8	-40.2	564	0.62	$1.8 \cdot 10^{-12}$	PKS 0306+102	J0309.1+1027	
128	10173	351.6	-40.2	648	0.70	$8.4 \cdot 10^{-11}$	PKS 2052-47	J2056.2-4715	P
129	10368	187.3	-43.4	339	0.39	$4.1 \cdot 10^{-15}$	PKS 0336-01	J0339.4-0144	
130	10386	239.5	-43.4	1411	1.54	$1.8 \cdot 10^{-50}$	PKS 0426-380	J0428.6-3756	P
131	10387	242.4	-43.4	440	0.48	$8.9 \cdot 10^{-7}$	PKS 0426-380	J0428.6-3756	P
132	10508	241.5	-45.0	683	0.75	$1.3 \cdot 10^{-6}$	PKS 0426-380	J0428.6-3756	P
133	10692	91.6	-48.1	289	0.32	$4.8 \cdot 10^{-9}$	PKS 2325+093	J2327.5+0940	P
134	10711	152.7	-48.1	569	0.63	$6.2 \cdot 10^{-22}$	MG1 J021114+1051	J0211.2+1050	P
135	10775	358.4	-48.1	582	0.64	$1.1 \cdot 10^{-12}$	MH 2136-428	J2139.3-4236	P
136	10779	11.7	-49.7	263	0.29	$1.2 \cdot 10^{-7}$	PMN J2145-3357	J2144.8-3356	
137	10840	215.0	-49.7	186	0.21	$1.1 \cdot 10^{-7}$	PKS 0347-211	J0350.0-2104	P
138	10847	238.3	-49.7	337	0.37	$3.5 \cdot 10^{-6}$	PKS 0402-362	J0403.9-3604	AT2413
139	10889	19.0	-51.3	1101	1.24	$6.0 \cdot 10^{-8}$	PKS 2155-304	J2158.8-3013	P
140	10965	282.1	-51.3	294	0.29	$2.9 \cdot 10^{-7}$	PKS 0235-618	J0237.1-6136	AT2669
141	10992	16.2	-52.8	1217	1.36	$2.2 \cdot 10^{-7}$	PKS 2155-304	J2158.8-3013	P
142	11131	163.1	-54.3	454	0.52	$7.3 \cdot 10^{-17}$	PKS 0215+015	J0217.9+0143	P
143	11495	213.7	-60.4	572	0.64	$5.2 \cdot 10^{-11}$	PKS 0301-243	J0303.4-2407	P
144	11506	263.2	-60.4	470	0.51	$9.1 \cdot 10^{-8}$	PKS 0244-470	J0245.9-4652	P
145	11572	210.8	-61.9	563	0.63	$1.9 \cdot 10^{-9}$	PKS 0250-225	J0252.7-2218	AT1933
146	11586	277.1	-61.9	625	0.67	$3.5 \cdot 10^{-13}$	PKS 0208-512	J0210.7-5102	P
147	11597	329.2	-61.9	267	0.28	$3.2 \cdot 10^{-11}$	PKS 2326-502	J2329.2-4956	AT2783
148	11598	333.9	-61.9	508	0.55	$1.5 \cdot 10^{-27}$	PKS 2326-502	J2329.2-4956	AT2783
149	11670	332.5	-63.5	805	0.87	$9.0 \cdot 10^{-62}$	PKS 2326-502	J2329.2-4956	AT2783
150	11680	23.8	-64.9	387	0.43	$2.1 \cdot 10^{-7}$	PKS 2255-282	J2258.0-2759	
151	11933	65.8	-70.9	953	1.09	$1.4 \cdot 10^{-90}$	PMN J2345-1555	J2345.0-1553	P

Table 2. List of sources with previously unreported variability. Additional columns describe source type: BL Lac (B), FSRQ (Q), AGN of uncertain type (AGN), or pulsar (PSR), the variability type: gradual increase or decrease in the photon flux rate (R), flares (F), or longer period of increased activity (A); in case of flares or activity, the temporal localization of events is given in the last column

Nº	Pixel №	l°	b°	N_{phot}	Φ_{-8}	P	Source	Type	Var.	Weeks
1	66	97.5	81.2	194	0.20	$3.9 \cdot 10^{-6}$	5C 12.291	Q	A	30–60
2	373	61.1	69.4	188	0.20	$1.8 \cdot 10^{-9}$	J1424+3615	B	A	140–160
3	564	108.5	64.9	201	0.19	$1.4 \cdot 10^{-7}$	CLASS J1333+5057	Q	R	—
4	1499	318.3	49.7	310	0.36	$8.1 \cdot 10^{-7}$	PMN J1332-1256	Q	R	—
5	1970	320.8	43.4	538	0.62	$8.3 \cdot 10^{-15}$	PMN J1344-1723	Q	R	—
6	2811	167.3	32.8	537	0.51	$9.6 \cdot 10^{-16}$	1ES 0806+524	B	R	—
7	2844	260.2	32.8	290	0.33	$1.3 \cdot 10^{-7}$	1RXS J102658.5-174905	B	R,F	176
8	2903	64.7	31.4	404	0.41	$2.1 \cdot 10^{-16}$	B2 1732+38A	B	F	40–50
9	3489	272.8	25.9	247	0.28	$1.3 \cdot 10^{-7}$	PKS B1043-291	Q	A	100–120
10	3540	57.7	24.6	557	0.58	$1.1 \cdot 10^{-16}$	RX J1754.1+3212	B	F	149–153
11	3598	220.8	24.6	439	0.50	$1.4 \cdot 10^{-7}$	PKS 0829+046	B	F	73
12	4000	270.0	20.7	325	0.36	$1.7 \cdot 10^{-15}$	PKS 1021-323	Q	R	—
13	4110	220.8	19.5	324	0.37	$2.0 \cdot 10^{-8}$	OJ 014	B	R	—
14	5165	308.0	9.6	1011	1.06	$2.6 \cdot 10^{-7}$	PMN J1326-5256	B	F	9.32
15	5637	195.5	4.8	52455	56.6	$2.3 \cdot 10^{-7}$	PSR J0633+1746	PSR	R	—
16	6608	46.4	-4.8	1198	1.3	$3.6 \cdot 10^{-7}$	RX J1931.1+0937	B	R	—
17	6711	336.1	-4.8	1717	1.8	$2.6 \cdot 10^{-9}$	PMN J1650-5044	Q	R	—
18	7101	351.6	-8.4	1553	1.71	$5.4 \cdot 10^{-38}$	PMN J1802-3940	Q	A	60–100
19	7155	144.8	-9.6	696	0.67	$3.4 \cdot 10^{-7}$	4C+47.08	B	A	100–140
20	7993	341.7	-17.0	512	0.54	$3.5 \cdot 10^{-6}$	PKS 1821-525	Q	R	—
21	8197	195.5	-19.5	896	1.01	$4.9 \cdot 10^{-20}$	TXS 0506+056	B	A	137–140, 169–172
22	8867	278.4	-25.9	508	0.50	$1.1 \cdot 10^{-13}$	PKS 0644-671	AGN	R	—
23	9197	128.0	-30.0	512	0.53	$1.1 \cdot 10^{-17}$	4C 31.03	Q	A	30–50, 148
24	10108	168.8	-40.2	564	0.62	$1.8 \cdot 10^{-12}$	PKS 0306+102	Q	F	141–147
25	10368	187.3	-43.4	339	0.39	$4.1 \cdot 10^{-15}$	PKS 0336-01	Q	F	131
26	10779	11.7	-49.7	263	0.29	$1.2 \cdot 10^{-7}$	PMN J2145-3357	Q	A	74, 91, 121
27	11680	23.8	-64.9	387	0.43	$2.1 \cdot 10^{-7}$	PKS 2255-282	Q	A	60–80, 136

a very bright flare of PKS 2255-282 in December 1997 [21]. Pulsed γ -rays from the Geminga pulsar were observed with 1 year of the Fermi-LAT data [22], while the source were considered nonvariable.

In this paper, the long-term flux change of the Geminga pulsar is detected with the KS probability $2.3 \cdot 10^{-7}$. In the present study, Geminga is the only pulsar demonstrating variability above our thresh-

old. For comparison, the respective KS probabilities for pixels containing Vela, PSR J1709-4429, and Crab pulsars are 25 %, 78 %, and 1.2 %. In the Crab case, it was shown that the observed variability is caused by processes in the Crab nebula rather than in the pulsar itself [23]. The Fermi-LAT collaboration also presented results of observations of three other gamma-ray pulsars (J1836+5925, PSR J2021+4026,

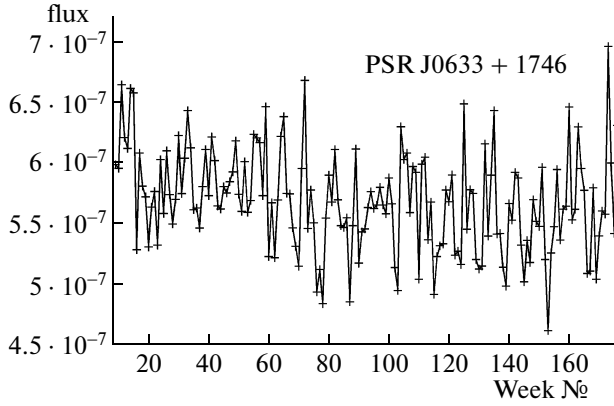


Fig. 4. The flux of photons with energies larger than 1 GeV for pixel № 5637 (Geminga). The flux is in $\text{photons} \cdot \text{cm}^{-2} \cdot \text{s}^{-1}$ units. The corresponding curves for all variable pixels listed in Table 2 are available at <http://arxiv.org/pdf/1201.3625v1>

and PSR J0007+7303) where no flux variability was observed [24–26].

According to 2FGL [14], an unaccounted instrumental effect may contribute to the apparent flux variability at the level of about 2 %. The effect may be related to the 55-day time scale corresponding to the precession of the LAT orbital plane. The systematic effect of this magnitude may be statistically significant for the brightest sources only, and therefore, among the sources in Table 2, only Geminga may be potentially affected. The observed variability of Geminga corresponds to a 7.2 % gradual flux decrease over 168 weeks. On the other hand, the KS test is not sensitive to the 55-day structure of the flux (integration over 8-week intervals does not significantly change the result). This is supported by the fact that the other bright pulsars do not show significant variability in our study, although they possess 55-day variations according to [14]. Still, we may not exclude that the apparent Geminga flux variability may be the result of unaccounted systematics on the 3-year time scale.

We note that while the 2FGL catalog contains 577 unidentified sources (out of 1873), 153 of which have the flux higher than $2 \cdot 10^{-9}$ $\text{photons} \cdot \text{cm}^{-2} \cdot \text{s}^{-1}$, none of them shows variability above our threshold.

It is also worth noting that sources not included in Table 2 because of being reported either in ATels or on the Fermi blog could have the variability patterns that differ considerably from the reported one. As an example, the flare from the source MG2 J130304+2434 that occurred on 3 July 2009 (week № 56) was reported in ATel #2110 [27]. On the other hand, Fig. 5 shows that

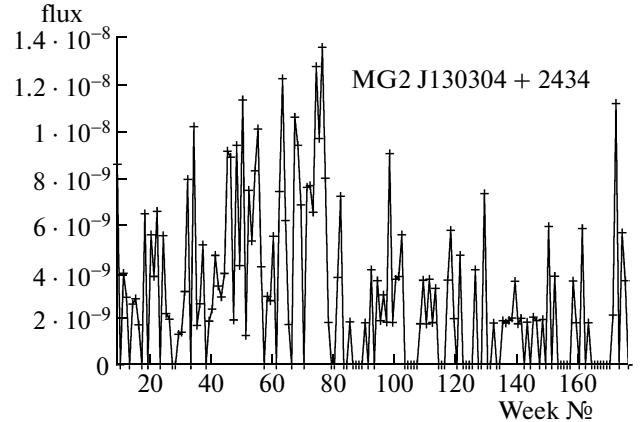


Fig. 5. The flux of photons with energies larger than 1 GeV for pixel № 23 (MG2 J130304+2434). Change of rate can be easily seen

the flare occurred during the high state of the source, with its flux slowly increasing from the start of the Fermi observations until approximately the 80th week when it began to decrease.

4. CONCLUSIONS

A method for detection of variable sources is proposed that uses the KS statistical test. The method is implemented for a full sky blind search for regions with variable flux at energies above 1 GeV using the Fermi-LAT 168 week data. The search leads to identification of 117 variable sources, the variability of 27 of which has not been reported before. Among the sources with previously unidentified variability, there are 25 AGNs belonging to the blazar class (11 BL Lacs and 14 FSRQs), one AGN of uncertain type (PKS 0644-671), and one pulsar PSR J0633+1746 (Geminga).

APPENDIX

The following ATels are cited in the text: ATel #1933 [28], ATel #2048 [29], ATel #2049 [30], ATel #2104 [31], ATel #2110 [27], ATel #2136 [32], ATel #2243 [33], ATel #2316 [34], ATel #2402 [35], ATel #2413 [36], ATel #2539 [37], ATel #2583 [38], ATel #2669 [39], ATel #2783 [40], ATel #2829 [41], ATel #2860 [42], ATel #2907 [43], ATel #2943 [44], ATel #3002 [45], ATel #3026 [46], ATel #3171 [47], ATel #3192 [20], ATel #3207 [48], ATel #3452 [16], ATel #3445 [49], ATel #3504 [19], ATel #3579 [15], ATel #3670 [50], ATel #3793 [51].

We are indebted to P. Tinyakov for the numerous helpful discussions at all stages of this work. We thank M. Gustafsson, B. Stern, I. Tkachev, and S. Troitsky for useful comments and suggestions. The work was supported in part by the RFBR grants 10-02-01406a, 11-02-01528a, 12-02-91323-SIGa (GR), 12-02-31776mol_a, 10-02-00961a, by the grants of the President of the Russian Federation NS-5525.2010.2 (GR), MK-1632.2011.2 (GR), MK-1582.2010.2 (MP), by the grant of the Government of Russian Federation 11.G34.31.0047(GR), and by the Ministry of Science and Education under contracts № 8412, 8525(GR). The work of MP is supported in part by the IISN project № 4.4509.10 and the Belgian Science Policy (IAP VI-11). GR is grateful for the hospitality to the ULB Service de Physique Théorique, where this study was initiated. The analysis is based on the data and software provided by the Fermi Science Support Center (FSSC). The numerical part of the work is performed at the cluster of the Theoretical Division of the INR, RAS. This research has made use of NASA's Astrophysics Data System and SIMBAD database, operated at CDS, Strasbourg, France.

REFERENCES

1. W. B. Atwood, A. A. Abdo, M. Ackermann et al., *Astrophys. J.* **697**, 1071 (2009); arXiv:0902.1089.
2. A. A. Abdo, M. Ackermann, M. Ajello et al., *Astrophys. J.* **722**, 520 (2010); arXiv:1004.0348.
3. M. T. Carini, H. R. Miller, J. C. Noble et al., *Astronom. J.* **101**, 1196 (1991).
4. M.-H. Ulrich, L. Maraschi, and C. M. Urry, *Ann. Rev. Astron. and Astrophys.* **35**, 445 (1997).
5. B. Y. Welsh, J. M. Wheatley, and J. D. Neil, *Astron. and Astrophys.* **527**, A15 (2011); arXiv:1101.2191.
6. B. Rani, P. J. Wiita, and A. C. Gupta , *Astrophys. J.* **696**, 2170 (2009); arXiv:0903.2606.
7. E. W. Bonning, C. Bailyn, C. M. Urry et al., *Astrophys. J.* **697**, L81 (2009); arXiv:0812.4582.
8. S. Soldi, M. Türler, S. Paltani et al., *Astron. and Astrophys.* **486**, 411 (2008); arXiv:0805.3411.
9. G. Ghisellini and F. Tavecchio, *MNRAS* **386**, L28 (2008); arXiv:0801.2569.
10. C. M. Raiteri, M. Villata, M. A. Ibrahimov et al., *Astron. and Astrophys.* **438**, 39 (2005); arXiv:astro-ph/0503312.
11. S. Ciprini, G. Tosti, C. M. Raiteri et al., *Astron. and Astrophys.* **400**, 487 (2003); arXiv:astro-ph/0301325.
12. C. M. Urry, L. Maraschi, R. Edelson et al., *Astrophys. J.* **411**, 614 (1993); arXiv:astro-ph/9304003.
13. K. M. Górski, E. Hivon, A. J. Banday et al., *Astrophys. J.* **622**, 759 (2005); arXiv:astro-ph/0409513.
14. The Fermi-LAT Collaboration, ArXiv e-prints (Aug. 2011), 1108.1435.
15. D. Gasparrini and S. Cutini, *The Astronomer's Telegram* **3579**, 1 (2011).
16. D. Donato and J. S. Perkins, *The Astronomer's Telegram* **3452**, 1 (2011).
17. Y. T. Tanaka, Ł. Stawarz, D. J. Thompson et al., *Astrophys. J.* **733**, 19 (2011); arXiv:1101.5339.
18. F. K. Schinzel, K. V. Sokolovsky, F. D'Ammando et al., *Astron. and Astrophys.* **532**, A150 (2011); arXiv:1107.2926.
19. L. Carrasco, A. Carraminana, G. Escobedo et al., *The Astronomer's Telegram* **3504**, 1 (2011).
20. M. Mariotti, *The Astronomer's Telegram* **3192**, 1 (2011).
21. D. J. Macomb, N. Gehrels, and C. R. Shrader, *Astrophys. J.* **513**, 652 (1999).
22. A. A. Abdo, M. Ackermann, M. Ajello et al., *Astrophys. J.* **720**, 272 (2010).
23. R. Buehler, J. D. Scargle, R. D. Blandford et al., arXiv:1112.1979.
24. A. A. Abdo, M. Ackermann, M. Ajello et al., *Astrophys. J.* **712**, 1209 (2010).
25. P. Saz Parkinson, W. Becker, A. Carramiñana et al., in *AAS/High Energy Astrophysics Division #11* (2010), vol. 42 of *Bulletin of the American Astronomical Society*, p. 679.
26. A. A. Abdo, K. S. Wood, M. E. DeCesar et al., *Astrophys. J.* **744**, 146 (2012); arXiv:1107.4151.
27. E. Hays and M. Marelli, *The Astronomer's Telegram* **2110**, 1 (2009).
28. S. Corbel and L. C. Reyes, *The Astronomer's Telegram* **1933**, 1 (2009).
29. S. Ciprini, *The Astronomer's Telegram* **2048**, 1 (2009).
30. S. Ciprini, *The Astronomer's Telegram* **2049**, 1 (2009).
31. F. Longo, G. Iafrate, E. Hays et al., *The Astronomer's Telegram* **2104**, 1 (2009).

32. S. Ciprini, The Astronomer's Telegram **2136**, 1 (2009).
33. Y. T. Tanaka, H. Takahashi, and S. E. Healey, The Astronomer's Telegram **2243**, 1 (2009).
34. E. Hays and L. Escande, The Astronomer's Telegram **2316**, 1 (2009).
35. K. V. Sokolovsky, F. K. Schinzel, and E. Wallace, The Astronomer's Telegram **2402**, 1 (2010).
36. A. B. Hill and J. Vandenbroucke, The Astronomer's Telegram **2413**, 1 (2010).
37. E. Wallace, The Astronomer's Telegram **2539**, 1 (2010).
38. D. Donato, The Astronomer's Telegram **2583**, 1 (2010).
39. S. Cutini, The Astronomer's Telegram **2669**, 1 (2010).
40. F. D'Ammando, The Astronomer's Telegram **2783**, 1 (2010).
41. F. K. Schinzel, The Astronomer's Telegram **2829**, 1 (2010).
42. F. D'Ammando, The Astronomer's Telegram **2860**, 1 (2010).
43. A. Cannon and F. D'Ammando, The Astronomer's Telegram **2907**, 1 (2010).
44. S. Ciprini, The Astronomer's Telegram **2943**, 1 (2010).
45. F. D'Ammando and J. Vandenbroucke, The Astronomer's Telegram **3002**, 1 (2010).
46. A. Allafort and F. D'Ammando, The Astronomer's Telegram **3026**, 1 (2010).
47. S. Buson and D. Bastieri, The Astronomer's Telegram **3171**, 1 (2011).
48. A. Allafort, The Astronomer's Telegram **3207**, 1 (2011).
49. D. Gasparrini, The Astronomer's Telegram **3445**, 1 (2011).
50. F. K. Schinzel and S. Ciprini, The Astronomer's Telegram **3670**, 1 (2011).
51. R. Ojha, M. Dutka, and E. Torresi, The Astronomer's Telegram **3793**, 1 (2011).